

Ordering process in the kinetic Ising model on the honeycomb lattice

Hiroshi Takano

Department of Physics, Faculty of Science and Technology, Keio University, Yokohama 223, Japan

Seiji Miyashita

Graduate School of Human and Environmental Studies, Kyoto University, Kyoto 606, Japan

(Received 9 February 1993)

The ordering process after quenching from infinite temperature is studied in the kinetic Ising model on the honeycomb lattice below the critical temperature by means of Monte Carlo simulations. Because of the presence of metastable droplets on the honeycomb lattice, the time scale of ordering becomes very long at low temperatures. Due to the metastability, the time evolution of magnetization per site, $m(t)$, seems to be scaled by a characteristic time scale $\exp(2K)L^{-2}t$ for large L . Here, K , L , and t denote the nearest-neighbor coupling divided by the temperature, the linear dimension of the system, and the time after the quenching, respectively.

I. INTRODUCTION

The dynamical properties of the kinetic Ising model with the nonconserved order parameter below the critical temperature have been attracting much attention. One interesting problem that has been studied is how the order grows after quenching from the disordered phase to the ordered phase.¹ Another interesting problem is how the autocorrelation function of a single spin decays in time in the equilibrium.² In both problems, it is understood that the dynamics of a droplet or a cluster, which is a domain of one ordered state in the background of the other ordered state, plays an important role for the long-time behavior of the system. Note that below the critical temperature there are two equivalent ordered states with positive and negative spontaneous magnetizations $\pm m_s$. The behavior of clusters is described by the motion of their surfaces or domain walls, which leads to the well-known k^2t scaling.¹

Let us define a cluster microscopically as a set of spins of the same sign which are connected by nearest-neighbor bonds. A cluster is called unstable against a single spin flip if the cluster can be eliminated or transformed into another cluster with lower energy by a series of single spin flips of which each flip does not increase the energy. All clusters of finite size are unstable against a single spin flip on most regular lattices such as the square lattice. On the honeycomb lattice, however, there are clusters which are metastable against the single spin flip. Namely, for such clusters, any transformation by a single spin flip requires an energy increase. An example of such clusters is shown in Fig. 1. Such a cluster cannot be eliminated by single spin flips at $T = 0$, where the spin flip with energy increase is not allowed. From the point of view of the distribution of relaxation rates of the kinetic Ising model,³ the presence of metastable clusters means that there are many relaxation modes, the relaxation rates of which approach zero as the temperature approaches

zero. It is an interesting problem how the presence of the many slow relaxation modes, which correspond to the metastable clusters, affects the dynamics in the ordered phase.

Generally, there are many systems with various types of metastable clusters. For example, there are metastable clusters in random Ising ferromagnets on any regular lattice.⁴ Furthermore, the nucleation process in an ordered state with an unfavorable field has been also studied.⁵ In the present model, clusters are metastable because of a local energy barrier for the domain-wall motion, which provides a type of metastability. Slow relaxation due to a similar type of metastability has been studied for the antiferromagnetic Ising models on the square lattice with nearest-neighbor and next-nearest-neighbor interactions⁶ and also for the Potts models.⁷

In this paper, we study the ordering process after

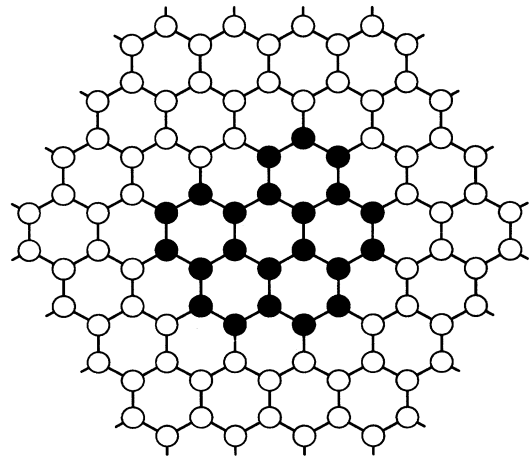


FIG. 1. Metastable cluster on the honeycomb lattice. Open and solid circles represent plus and minus spins, respectively.

quenching from the disordered phase to the ordered phase by the Monte Carlo method. By comparing the results for the honeycomb and square lattices, we clarify the effect of the presence of metastable clusters. In Sec. II, the model and method are explained. The results of Monte Carlo simulations are presented in Sec. III. Summary and discussion are given in the last section

II. MODEL AND METHOD

In this paper, we consider the kinetic Ising model on the honeycomb and square lattices. The Hamiltonian of the system including the factor $-1/(k_B T)$, where k_B and T are the Boltzmann constant and the temperature, respectively, is given by

$$\mathcal{H} = -\frac{1}{k_B T} H = \frac{J}{k_B T} \sum_{\langle i,j \rangle} S_i S_j = K \sum_{\langle i,j \rangle} S_i S_j. \quad (1)$$

Here, $S_i = \pm 1$ denotes an Ising spin at the i th site and $\sum_{\langle i,j \rangle}$ denotes the summation over all the nearest-neighbor pairs. In the single-spin-flip kinetic Ising model, the probability $P(S;t)$ that the system has a spin configuration $S = \{S_j\}$ at time t obeys a master equation

$$\frac{\partial}{\partial t} P(S;t) = \sum_i [-W_i(S)P(S;t) + W_i(F_i S)P(F_i S;t)], \quad (2)$$

where $F_i S$ denotes a spin configuration obtained from S by flipping the i th spin. The transition probability per unit time $W_i(S)$ for the i th spin to flip in a configuration S is chosen to be of Glauber type:⁸

$$W_i(S) = \frac{1}{2}(1 - S_i \tanh E_i), \quad (3)$$

with

$$E_i = K \sum_j^{(i)} S_j, \quad (4)$$

where $\sum_j^{(i)}$ denotes the summation over all nearest-neighbor sites of the i th site. We use a continuous-time Monte Carlo method in order to simulate the master equation (2).⁹ The unit time in (2) corresponds to one Monte Carlo step per spin (MCS) in the usual Monte Carlo method.

For the honeycomb lattice, simulations are performed on systems consisting of spins contained in an equilateral hexagon of which each side intersects L nearest-neighbor bonds. The number of the spins in the hexagon is $6L^2$. For the square lattice, we consider L^2 spins in a square of which each side intersects L bonds. For both lattices, spins outside the hexagon or the square are assumed to be fixed to $+1$. The values of L used in the present simulations are $L = 4 - 64$ and $L = 8 - 96$ for the honeycomb and square lattices, respectively.

The coupling constant K is quenched from $K = 0$ (infinite temperature) to $K > K_c$ (below the critical temperature) at time $t = 0$, where K_c denotes the critical coupling. The values of K used for the honeycomb lattice are $K = 4$ and 6 ($K_c \simeq 0.66$), and those for the square lattice are $K = 2$ and 4 ($K_c \simeq 0.44$). A sam-

ple of an initial spin configuration, which corresponds to $K = 0$, is prepared by assigning a value $+1$ or -1 randomly for each spin. Then, the Monte Carlo method is applied to generate a sample of the time evolution of the spin configuration described by the master equation (2) with the coupling constant $K > K_c$ until the magnetization reaches the equilibrium value m_s . For example, for the honeycomb lattice with $L = 96$ at $K = 6$, we performed the simulation until $t = 10^9$ MCS. The obtained time sequence of spin configurations gives a sample $S(t)$ of the stochastic process. This process is repeated for 10^4 samples of the initial state for each set of values of L and K . The set of samples $\{S(t)\}$ thus obtained serves as $P(S;t)$. Therefore, the averages with respect to $P(S;t)$ can be estimated from the averages over the samples of $S(t)$. As an example, let us consider a physical quantity $A(S)$, which is a function of the spin configuration S . The average of $A(S)$ with respect to $P(S;t)$ is defined as

$$\langle A(t) \rangle = \sum_S A(S) P(S;t). \quad (5)$$

In the simulation, this average is estimated as the average of $A(S(t))$ over the samples of $S(t)$:

$$\langle A(t) \rangle = \frac{\sum_{S(t)} A(S(t))}{\sum_{S(t)} 1}. \quad (6)$$

III. RESULTS OF MONTE CARLO SIMULATIONS

Let us consider the time dependence of the magnetization per site m , which is defined as

$$m = \frac{1}{N} \sum_i S_i, \quad (7)$$

for a system of N spins. Figure 2 shows the time dependence of $\langle m(t) \rangle$ for the square lattice with $K = 4$. The results for the square lattice with $K = 2$ are almost the same as those for $K = 4$ and are not shown here. Figures 3(a) and 3(b) show the results for the honeycomb lattice with $K = 4$ and $K = 6$, respectively. Note that the positive values of $\langle m(t) \rangle$ result from the boundary condition that spins outside of the system are fixed to $+1$. If the free-boundary condition is adopted, namely,

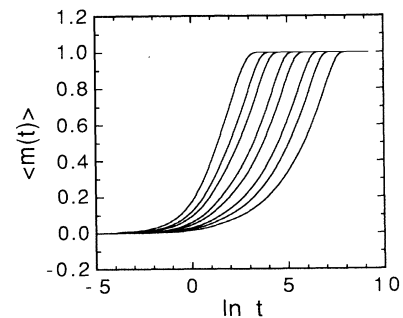


FIG. 2. Time dependence of $\langle m(t) \rangle$ for the square lattice with $K = 4$. From left to right, the lines correspond to $L = 8, 12, 16, 24, 32, 48, 64, 96$, respectively.

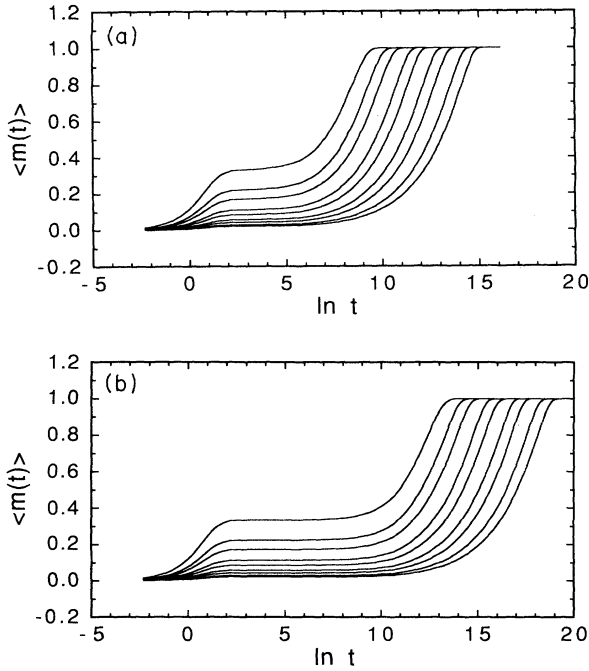


FIG. 3. Time dependence of $\langle m(t) \rangle$ for the honeycomb lattice with (a) $K = 4$ and (b) $K = 6$. From left to right in each figure, the lines correspond to $L = 4, 6, 8, 12, 16, 24, 32, 48,$ and 64 , respectively.

if the outside spins are absent, $\langle m(t) \rangle$ is zero. In Fig. 3, the plateau behavior of $\langle m(t) \rangle$ is clearly seen for the time region around $\ln t \sim 3$. Before the plateau time region, $\langle m(t) \rangle$ for each L shows little K dependence. The plateau behavior is considered to result from the metastability of clusters, which has longer lifetime at lower temperatures. The time dependence of the magnetization for a sample $S(t)$, which is denoted by $m(S(t))$, is shown in Fig. 4 for $L = 8$ with $K = 4$. Actually, $m(S(t))$ does not change in a certain time region corresponding to the plateau behavior. This means that the configuration itself does not change in this time region. In Fig. 5, the spin configuration in this time region is shown together with the initial configuration for this sample $S(t)$. This figure shows that in the plateau time region the spin configuration consists of metastable clusters.

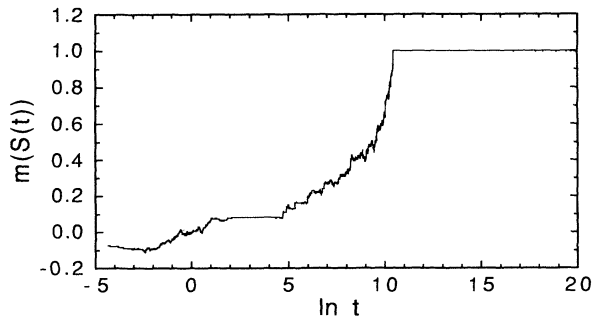


FIG. 4. Time dependence of the magnetization of a sample $S(t)$ for the honeycomb lattice with $L = 8$ and $K = 4$.

In order to see that the plateau behavior comes from the metastable states, we analyze the local field acting on each spin. Let us define a normalized local energy ℓ_i for a spin S_i at site i as

$$\ell_i = S_i \sum_j^{(i)} S_j = S_i E_i / K. \quad (8)$$

The possible values of ℓ_i are $\{-4, -2, 0, 2, 4\}$ for the square lattice and $\{-3, -1, 1, 3\}$ for the honeycomb lattice. Let N_ℓ denote the number of spins for which the local energy $\ell_i = \ell$:

$$N_\ell = \sum_i \delta_{\ell_i, \ell}. \quad (9)$$

The density of such spins are given by

$$n_\ell = N_\ell / N. \quad (10)$$

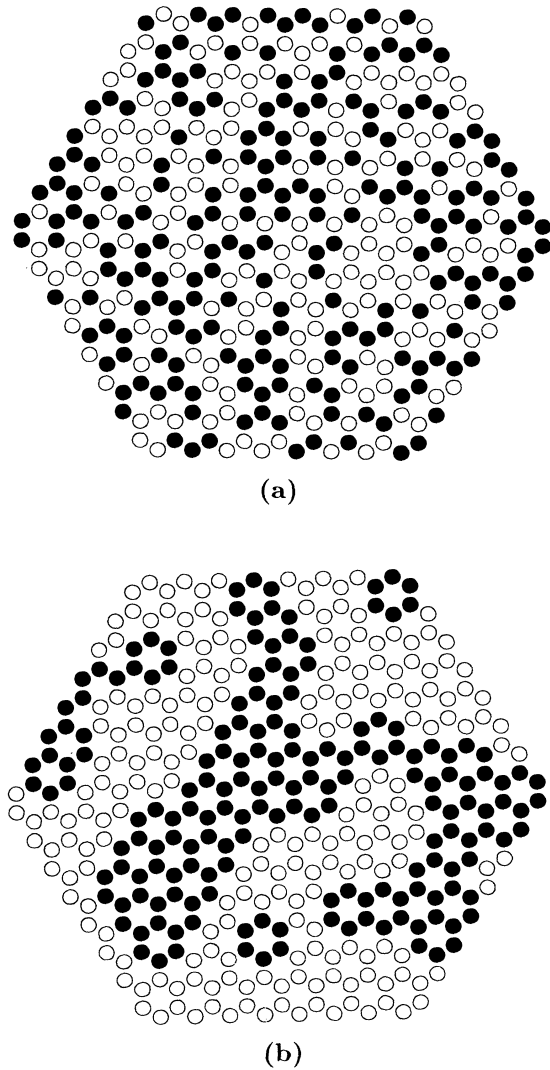


FIG. 5. Spin configurations in a sample $S(t)$. The sample is same as that shown in Fig. 4. The configuration at $t = 0$ is shown in (a), and that in the plateau time region is shown in (b).

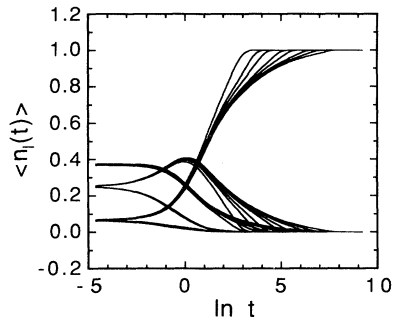


FIG. 6. Time dependence of $\langle n_\ell(t) \rangle$ for the square lattice with $K = 4$. From top to bottom at time around $\ln t \sim -4$, the bundles of lines correspond to $\ell = 0, 2, -2, 4$, and -4 , respectively. From left to right within each bundle, the lines correspond to $L = 8, 12, 16, 24, 32, 48, 64$, and 96 , respectively.

Figure 6 shows $\langle n_\ell(t) \rangle$ for the square lattice with $K = 4$. Again, the results for $K = 2$ are almost the same. We can see that $\langle n_{-4}(t) \rangle$ and $\langle n_{-2}(t) \rangle$ show little L dependence and become almost zero after a short time. After then, $\ell_i = 0, 2$, or 4 for almost all spins. The value $\ell_i = 0$ corresponds to spins at the corners of clusters, $\ell_i = 2$ to those on the flat edges of clusters, and $\ell_i = 4$ to those inside the ordered region. This means that the relevant spin configurations consist of clusters with flat surfaces at the late stage, as expected. Figures 7(a) and 7(b) show

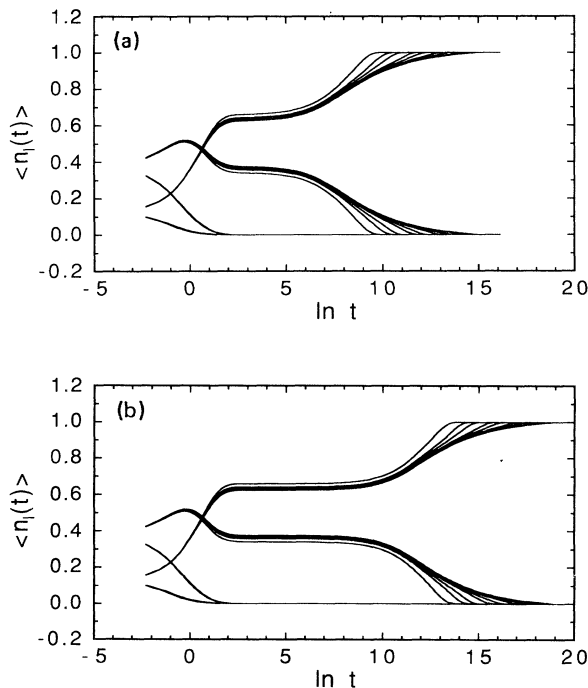


FIG. 7. Time dependence of $\langle n_\ell(t) \rangle$ for the honeycomb lattice with (a) $K = 4$ and (b) $K = 6$. From top to bottom at time around $\ln t \sim -2$, the bundles of lines correspond to $\ell = 1, -1, 3$, and -3 , respectively. From left to right within each bundle, the lines correspond to $L = 4, 6, 8, 12, 16, 24, 32, 48$, and 64 , respectively.

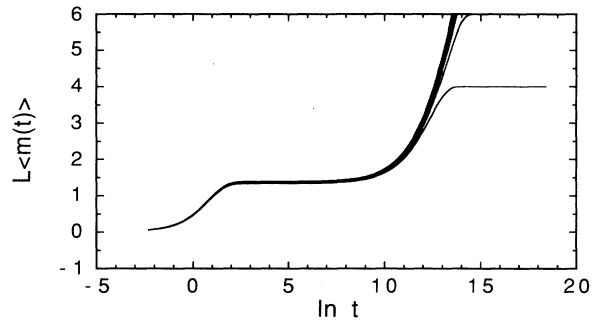


FIG. 8. Time dependence of $L\langle m(t) \rangle$ for the honeycomb lattice with $K = 6$. The data for $L = 4, 6, 8, 12, 16, 24, 32, 48$, and 64 are shown.

$\langle n_\ell(t) \rangle$ for the honeycomb lattice with $K = 4$ and 6 , respectively. It can be seen that the dependence of $\langle n_{-3}(t) \rangle$ and $\langle n_{-1}(t) \rangle$ on K and L is small. In the plateau time region, almost all spins have $\ell_i = 1$ or $\ell_i = 3$. This means that the configurations in the plateau time region consist of metastable clusters. In this time region, $\langle n_1(t) \rangle$ and $\langle n_3(t) \rangle$ also show plateau behavior. Thus, the plateau behavior can be regarded as a result of the metastability of the configurations.

The ordering process on the honeycomb lattice can be summarized as follows. There seems to be three time regions divided by two characteristic times t_1 and t_2 . For $t < t_1$, the numbers of sites with $\ell_i = -1$ or -3 decrease and $\langle m(t) \rangle$ approaches a plateau value. The dependence of t_1 on K and L is small. For $t_1 < t < t_2$, $\langle m(t) \rangle$ shows a plateau, which results from the configurations consisting of metastable clusters. The value of t_2 is larger for larger values of K and L . The plateau values of $\langle m(t) \rangle$ seem to be proportional to $1/L$. See Fig. 8, where $L\langle m(t) \rangle$ versus $\ln t$ is shown. This can be interpreted as follows. Formation of metastable clusters occurs locally. The clusters formed near the boundary of the system are affected by the surrounding $+$ spins. There, spins tend to be $+$. The number of such spins is proportional to L . Thus the metastable configuration at the plateau has a total magnetization proportional to L . Because the number of spins in the system is proportional to L^2 , the mag-

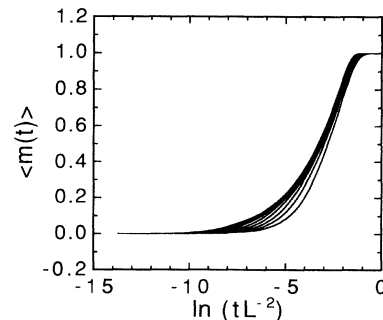


FIG. 9. Plot of $\langle m(t) \rangle$ vs $\ln(tL^{-2})$ for the square lattice with $K = 4$. The data for $L = 8, 12, 16, 24, 32, 48, 64$, and 96 are shown.

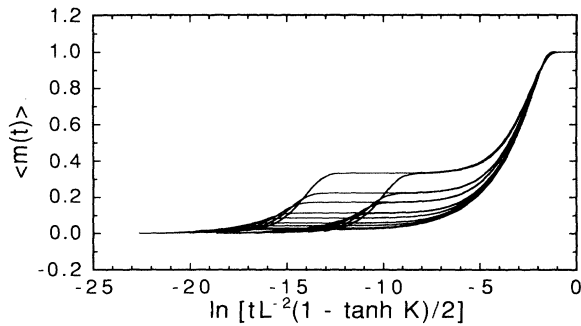


FIG. 10. Plot of $\langle m(t) \rangle$ vs $\ln [tL^{-2}(1 - \tanh K)/2]$ for the honeycomb lattice with $K = 4$ and 6 . The data for $L = 4, 6, 8, 12, 16, 24, 32, 48,$ and 64 are shown.

netization per spin should be proportional to $1/L$. The time region $t_2 < t$ is the final stage of the ordering process, where $\langle m(t) \rangle$ changes from the plateau value to its equilibrium value $\langle m(\infty) \rangle = m_s \simeq 1$. In this time region, n_1 decreases, which corresponds to decrease of the surface length of the metastable clusters. The curves of $\langle m(t) \rangle$ seem to have similar shapes around $\langle m(t) \rangle \sim 1$. They seem to collapse into a single curve through the translation along the $\ln t$ axis. The scaling analysis of the behavior of $\langle m(t) \rangle$ in this time region is given in the following.

Generally, the k^2t scaling¹ is known to hold for the time dependence of the structure function in the late stage of the ordering process. From this scaling, it is expected that the t/L^2 scaling holds for the behavior of $\langle m(t) \rangle$ in the present model as well. Figure 9 shows the scaling plot $\langle m(t) \rangle$ versus $\ln(tL^{-2})$ for the square lattice with $K = 4$. The difference between the results for $K = 2$ and $K = 4$ is small. The scaling seems to hold at the late stage of the ordering for larger L . In the case of the honeycomb lattice, the metastable clusters remain at the late stage. In order to change the configuration, spins with $\ell_i = 1$ should be flipped. Thus, it is necessary to include the transition rate of spins with $\ell_i = 1$ into the time scaling variable. This transition rate is given by

$$\begin{aligned} W_i(S) &= \frac{1}{2}(1 - S_i \tanh E_i) = \frac{1}{2}(1 - \tanh S_i E_i) \\ &= \frac{1}{2}(1 - \tanh K\ell_i) = \frac{1}{2}(1 - \tanh K). \end{aligned} \quad (11)$$

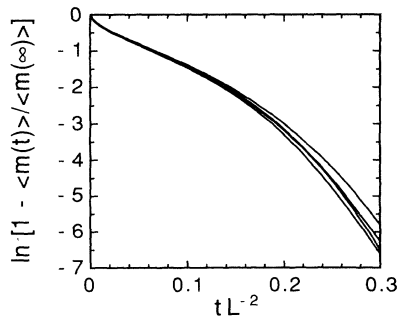


FIG. 11. Plot of $\ln [1 - \langle m(t) \rangle / \langle m(\infty) \rangle]$ vs tL^{-2} for the square lattice with $K = 4$. The data for $L = 32, 48, 64,$ and 96 are shown.

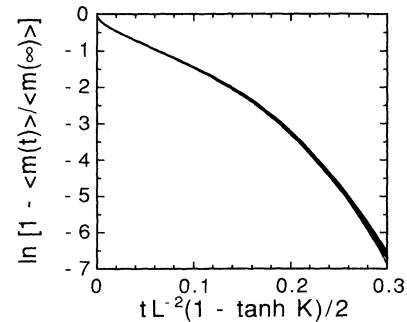


FIG. 12. Plot of $\ln [1 - \langle m(t) \rangle / \langle m(\infty) \rangle]$ vs $tL^{-2}(1 - \tanh K)/2$ for the honeycomb lattice with $K = 4$ and 6 . The data for $L = 24, 32, 48,$ and 64 are shown.

Figure 10 shows the scaling plot $\langle m(t) \rangle$ versus $\ln [tL^{-2}(1 - \tanh K)/2]$ for the honeycomb lattice with $K = 4$ and $K = 6$. The data collapse well to a scaling function at the late stage. In order to see the scaling behavior of $\langle m(t) \rangle$ in more detail, $\ln [1 - \langle m(t) \rangle / \langle m(\infty) \rangle]$ versus tL^{-2} is shown in Fig. 11 for the square lattice with $L \geq 32$ and $\ln [1 - \langle m(t) \rangle / \langle m(\infty) \rangle]$ versus $tL^{-2}(1 - \tanh K)/2$ is shown in Fig. 12 for the honeycomb lattice with $L \geq 24$. Here, the equilibrium value $\langle m(\infty) \rangle$ is approximately given by $1 - 2 \exp(-8K) - (8 - 8/L) \exp(-12K)$ and $1 - 2 \exp(-6K) - (6 - 2/L) \exp(-8K)$ for the square and honeycomb lattices, respectively. These formulas are obtained by the low temperature expansion on a finite lattice.¹⁰

IV. SUMMARY AND DISCUSSIONS

In this paper, the ordering processes of the ferromagnetic Ising model on the honeycomb lattice are studied. Because of the existence of the metastable clusters, the time evolution of the magnetization $\langle m(t) \rangle$ shows a plateau. After the plateau time region, metastable configurations remain. In order to reach the equilibrium state, a process which increases the energy $2J$ is inevitable. Thus, the time scale of the process becomes of activation type, $\exp(2K)$, which corresponds to the transition rate $\frac{1}{2}(1 - \tanh K)$, Eq. (11). This makes the ordering processes very slow, which is not observed in the square lattice, where all clusters are unstable.

However, it should be noted that the ordering process at late stage also follows the k^2t scaling. This means that if the time scale is normalized appropriately, the motion of the domain wall on the honeycomb lattice is essentially the same as that on the square lattice. In general, if the energy barrier of the metastability has an upper bound and the system can be regarded to be uniform at a certain length scale, then the k^2t scaling is expected to hold with a properly normalized time scale.

Similar slow ordering processes are expected for the Penrose lattice, where metastable clusters also exist.

As mentioned in Sec. I, there are various types of metastability. In many cases, the time evolution of the system becomes very slow due to the metastability, where

the dynamics of the domain wall is discussed to be different from the ordinary type of k^2t scaling.¹¹ The present observation suggests that such an essentially slow relaxation should be attributed to the existence of an arbitrarily large energy barrier with nonzero probability. It would be interesting to classify the types of such non-ordinary ordering processes from the point of view of the distribution of the energy barrier of the metastable states.

ACKNOWLEDGMENTS

The authors would like to thank Professor A. Jacobs who pointed out the existence of the metastable clus-

ters on the honeycomb lattice. Part of the present work had been done while one of the authors (H.T.) was visiting Cavendish Laboratory, the University of Cambridge. He wishes to thank the members of the Theory of Condensed Matter group at Cavendish Laboratory for their hospitality. The authors thank the Institute of Statistical Mathematics and the University of Cambridge for the computer facilities. The present work was partially supported by a Grant-in Aid for Scientific Research on Priority Areas, Computational Physics as a New Frontier in Condensed Matter Research, from the Ministry of Education, Science and Culture.

-
- ¹T. Ohta, D. Jasnow, and K. Kawasaki, *Phys. Rev. Lett.* **49**, 1223 (1982); P. S. Sahni, G. Dee, J. D. Gunton, M. Phani, J. L. Lebowitz, and M. Kalos, *Phys. Rev. B* **24**, 410 (1981); J. D. Gunton, M. San Miguel, and P. S. Sahni, in *Phase Transitions and Critical Phenomena*, edited by C. Domb and J. L. Lebowitz (Academic, London, 1983), Vol. 8.
- ²H. Takano and H. Nakanishi, and S. Miyashita, *Phys. Rev. B* **37**, 3716 (1988); D. A. Huse and D. S. Fisher, *ibid.* **35**, 6841 (1987).
- ³S. Miyashita and H. Takano, *Prog. Theor. Phys.* **73**, 1122 (1985).
- ⁴A. E. Jacobs and C. M. Coram, *Phys. Rev. B* **36**, 3844 (1987); M. Cieplak and T. R. Gawron, *J. Phys. A* **20**, 5657 (1987); T. Kawasaki, *Prog. Theor. Phys.* **80**, 203 (1988); **84**, 213 (1990); S. Miyashita and T. Kawasaki, in *Slow Dynamics in Condensed Matter*, Proceedings of the Conference on Slow Dynamics in Condensed Matter, AIP Conf. Proc. No. 256, edited by K. Kawasaki, M. Tokuyama, and T. Kawakatsu (AIP, New York, 1992); T. Kawasaki and S. Miyashita, *Prog. Theor. Phys.* **89**, 985 (1993).
- ⁵K. Binder and M. Müller-Krumbhaar, *Phys. Rev. B* **9**, 2328 (1974); H. Tomita and S. Miyashita, *ibid.* **46**, 8886 (1992).
- ⁶A. Høst-Madsen, P. J. Shah, T. V. Hansen, and O. G. Mouritsen, *Phys. Rev. B* **36**, 2333 (1987); O. G. Mouritsen, H. C. Fogedby, and E. Paestgaard, in *Dynamics of Ordering Processes in Condensed Matter*, edited by S. Komura and H. Furukawa (Plenum, New York, 1988); J. D. Shore and J. P. Sethna, *Phys. Rev. B* **43**, 3782 (1991).
- ⁷J. Viñals and J. D. Gunton, *Phys. Rev. B* **33**, 7795 (1986); J. Viñals and M. Grant, *ibid.* **36**, 7036 (1987); P. S. Sahni, D. J. Srolovitz, G. S. Grest, M. P. Anderson, and S. A. Safran, *ibid.* **28**, 2705 (1983); G. S. Grest, M. P. Anderson, and D. J. Srolovitz, *ibid.* **38**, 4752 (1988).
- ⁸R. J. Glauber, *J. Math. Phys.* **4**, 294 (1963).
- ⁹A. B. Bortz, M. H. Kalos, and J. L. Lebowitz, *J. Comput. Phys.* **17**, 10 (1975); S. K. Ma, *Phys. Rev. Lett.* **37**, 461 (1976); K. Binder, in *Monte Carlo Methods in Statistical Physics*, edited by K. Binder (Springer, Berlin, 1979); J. C. Angles d'Auriac, R. Maynard, and R. Rammal, *J. Stat. Phys.* **28**, 307 (1982); H. Takano, *Prog. Theor. Phys.* **68**, 493 (1982).
- ¹⁰C. Domb, in *Phase Transitions and Critical Phenomena*, edited by C. Domb and M. S. Green (Academic, London, 1974), Vol. 3.
- ¹¹D. A. Huse and C. L. Henly, *Phys. Rev. Lett.* **54**, 2708 (1985); A. J. Bray and K. Humayun, *J. Phys. A* **24**, L1185 (1991); H. Hayakawa, *J. Phys. Soc. Jpn.* **60**, 2492 (1991); S. Puri and N. Parekh, *J. Phys. A* **25**, 4127 (1992).